Mechanics of Materials 42 (2010) 1031–1042

Contents lists available at ScienceDirect

Mechanics of Materials

journal homepage: www.elsevier.com/locate/mechmat

Fracture characterization of concrete/epoxy interface affected by moisture

Denvid Lau, Oral Büyüköztürk *

Department of Civil and Environmental Engineering, Massachusetts Institute of Technology, Cambridge, MA 02139, USA

ARTICLE INFO

Keywords:
Concrete
Debonding
Epoxy
Fracture
Interface
Moisture

ABSTRACT

Knowledge on durability of concrete/epoxy bonded systems is becoming essential as the use of these systems in applications such as fiber-reinforced polymer (FRP) in strengthening of concrete structures is becoming increasingly popular. Prior research studies in this area indicate that moisture plays an important role on durability of these systems. Premature failures of the bonded system may occur regardless of the durability of the individual constituent materials forming the material system, and that the durability of the overall FRP-bonded system may be governed by the interface integrity. In this study, fracture toughness of concrete/epoxy interfaces as affected by combinations of various degrees of moisture ingress and temperature levels is quantified. For this purpose, sandwiched beam specimens containing concrete/epoxy interfaces were tested and analyzed using the concepts of fracture mechanics. Mechanical properties of individual materials constituting the interface (concrete and epoxy) were also characterized for the evaluation of the corresponding interface fracture toughness. Experimental results have shown a significant decrease, up to about 50%, in the interface fracture toughness of concrete/epoxy bond with selected levels of moisture and temperature conditioning of the specimens for both mode I and mixed mode conditions, and that moisture affected debonding may occur in the interface region involving a distinctive dry-to-wet debonding mode shift from material decohesion (concrete delamination) to interface separation. The mechanistic knowledge and the experimental data presented in this paper will serve as a basis for the use in the design improvement of material systems containing such interfaces for better system durability.

1. Introduction and objective

Layered composites consisting of dissimilar materials are used at different length-scales in various structural applications. Thin film coated elements for various purposes are examples of small-scale applications. A fiber-reinforced polymer (FRP)-bonded concrete system which is a multi-layer material consisting of FRP, epoxy and concrete is a larger-scale application (Buyukozturk and Hearing, 1998a). In this system, the interface between concrete and epoxy is usually regarded to be stronger when compared to the strength of the concrete substrate as found in many existing data on the failure of FRP-bonded concrete beams (Teng et al., 2002). This is generally true when the interface is under dry conditions, as evidenced by the experiments. However, the durability of such a bi-material system under moisture conditions is yet to be understood.

Interfacial degradation may be quantified through a strength-based or a fracture-based approach. Strength-based models, based on interfacial stress, strength, and surface interlocking concepts (Smith and Teng, 2001; Frigione et al., 2006), have been widely used to predict the global debonding failure of bi-layer material systems. However, such an approach intrinsically neglects the failure process of local debonding regions, which is closely related to the fracture properties of the bi-material system. Interface fracture toughness, which is a bond property in a

* Corresponding author. Tel.: +1 617 253 7186; fax: +1 617 253 3479.
E-mail addresses: denvid@mit.edu (D. Lau), obuyuk@mit.edu (O. Büyüköztürk).

0167-6636/$ - see front matter © 2010 Elsevier Ltd. All rights reserved.
doi:10.1016/j.mechmat.2010.09.001

bi-layer material system, can be used to quantify the resistance to crack initiation in local regions, and to predict the crack propagation based on the kink criterion (He and Hutchinson, 1989). Fracture-based mechanics tests aim at determining the fracture toughness (Γ) required to produce the debonding failure in a bi-layer material system. Different fracture-based test procedures have been proposed for the determination of bond properties of composite layered materials. Detailed discussions of these procedures and their applicability for predicting the bond behavior can be found in various publications (Taljsten, 1996; Buyukozturk and Hearing, 1998b; Giurgiutiu et al., 2001; Buyukozturk et al., 2004; Qiao and Xu, 2004; Yuan et al., 2004; Au and Büyüköztürk, 2006a,b; Coronado and Lopez, 2008; Gunes et al., 2009; Lau and Buyukozturk, 2009).

In order to evaluate the interface fracture toughness in a bi-layer material system, several key material properties are required beforehand, namely, the Young's modulus and the Poisson's ratio of the constituent materials. Also, the fracture toughness of the substrate should be obtained for investigating the behavior of such system after crack initiation. The effect of moisture on the mechanical properties of concrete has been investigated by a number of research groups (Bazant and Thonguthai, 1978; Bazant and Prat, 1988; Ross et al., 1996; Konvalinka, 2002). Related research works have concluded that the mechanical properties of concrete, including mode I fracture toughness and compressive strength, degrade with increasing moisture content in general (Bazant and Thonguthai, 1978; Ross et al., 1996). However, there is a need for further quantification of how moisture and temperature affect fracture initiation and propagation until failure in concrete. Material properties of epoxy vary significantly among different types of epoxy. Also, the extent of the effect of moisture on its mechanical properties is highly variable for different epoxy types. With such uncertainty on its mechanical properties, a comprehensive characterization of moisture affected properties of the epoxy in the bi-material system is very important.

To study the bonding between FRP and concrete, fracture tests using modified double cantilever beams (MDCB) were usually adopted (Karbhari and Engineer, 1996; Karbhari et al., 1997; Wan et al., 2006; Ouyang and Wan, 2008, 2009). With these specimens, loads can be applied easily at the end of FRP strips. However, the interface fracture energy estimated by these tests was often an order of magnitude higher than the fracture energy of the concrete substrate. In fact, the normal peel test involving primarily bending of the film may not be representative in quantifying the interface fracture energy of the bonded system because of various factors such as plasticity in the vicinity of the crack tip due to bending. The four-point bending and shear tests on sandwiched beam specimens have been shown to be robust in quantifying the interface fracture toughness in bi-layer materials, and thus, have been adopted in this research. These tests can be used for the determination of the mode I and mixed mode fracture toughnesses at the interface of a bi-material system (Lee and Buyukozturk, 1992, 1995; Trende and Buyukozturk, 1998) by incorporating the relationship between the interface fracture toughness and the phase angle.

The objective of this paper is to understand the effect of moisture on debonding in concrete/epoxy systems through a comprehensive characterization of the concerned interface and its constituent materials by means of an interface fracture approach. Experimental investigation on the mechanical properties of both concrete and epoxy, as well as a combined experimental/analytical approach for the determination of the interface fracture toughness is described. The study also focuses on the debonding mechanism along the interface once the debonding is initiated.

2. Scope of work

The work reported in this paper involves mainly experimental study. It consists of two main parts, namely, (i) mechanical property characterization of concrete and epoxy, and (ii) characterization of concrete/epoxy interface. In part (i), the compressive strength, the Young's modulus, mode I and mode II fracture toughnesses of concrete, as well as the tensile strength and the Young's modulus of epoxy were determined under different moisture content and temperatures. Equipped with the mechanical properties of concrete and epoxy from part (i), in part (ii) the mode I and mixed mode interface fracture toughnesses were calculated through the sandwiched beam specimens under consistent moisture and temperature conditioning. Fracture toughnesses are used as key parameters to study the interfacial crack initiation, and to investigate debonding and crack propagation using the concept of kink criterion (He and Hutchinson, 1989).

3. Constituent materials: concrete and epoxy

Based on previous findings, the variation of Poisson's ratio under the effect of moisture may be considered insignificant (Bazant and Prat, 1988; Ross et al., 1996). Hence, the constant values of Poisson ratios for concrete and epoxy are used in this paper. The Young's modulus and compressive strength of concrete, and the Young's modulus and tensile strength of epoxy were measured from uniaxial tests. When studying the crack propagation along the interface between two materials, the fracture toughness of the substrate is required, and thus, the mode I and mode II fracture toughnesses of concrete were also obtained. To determine the compressive strength and the Young's modulus of concrete with increasing moisture content, compressive tests were performed in accordance to ASTM C39. The mode I and mode II fracture toughnesses of concrete were quantified by fracture tests which are commonly adopted in this field (Bazant and Prat, 1988; Reinhardt and Xu, 1998). The tensile strength and Young's modulus of epoxy were characterized in accordance to ASTM D638.

3.1. Specimens

Normal strength concrete of Grade 40 (95% of the tested concrete samples have strength above 40 N/mm^2) was used in this research. The maximum aggregate size was 10 mm. There were three different types of specimens for the mechanical characterization of concrete. Cylinder

specimens with dimensions of 50 mm (diameter) × 100 mm (height) were tested under uniaxial compression according to ASTM C39 in order to find the compressive strength and the Young's modulus of concrete. Mode I fracture beam specimens with dimensions of 100 mm (length) × 37.5 mm (height) × 37.5 mm (thickness) and a through thickness center notch that was 6.25 mm deep × 1.6 mm wide (see Fig. 1) were tested under mode I fracture condition based on prior research recommendations (Bazant and Prat, 1988). Span length of the fracture beam specimens was 93.75 mm which was 2.5 times the beam height. Mode II fracture block specimen with dimensions of 200 mm (width, $2w$) × 200 mm (height, $2h$) × 100 mm (thickness) and a through thickness double-edged notch with a depth 50 mm (see Fig. 2) based on recommendation from prior research studies (Xu et al., 1995; Reinhardt et al., 1997) were tested under mode II fracture condition.

A commercial two-component 100% solids nonsag epoxy was employed in this study. This epoxy is commonly adopted in current construction industry as a concrete bonding adhesive. The test data for this epoxy as provided by the manufacturer is shown in Table 1. It should be mentioned that the heat deflection temperature (HDT) 53 °C is an indication of the glass transition temperature T_g.

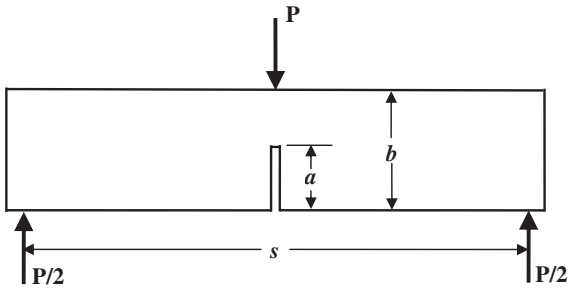

Fig. 1. Schematic diagram of a three-point bending setup.

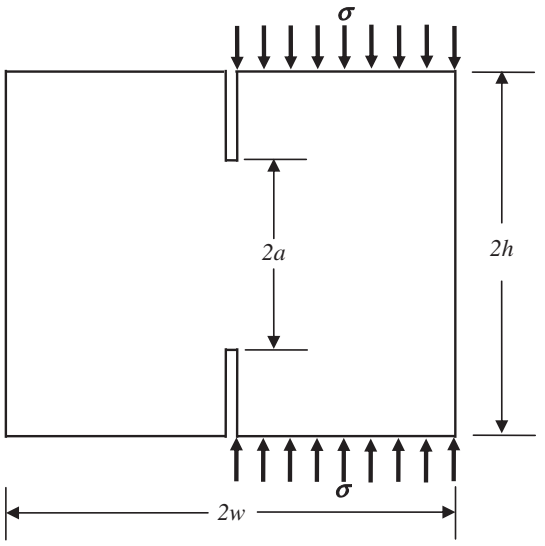

Fig. 2. Double-edged notch plate geometry.

Table 1
Mechanical properties of the epoxy as provided by the manufacturer.

Property	Result	Test method
Tensile strength (MPa)	13.8	ASTM D638
Young's modulus (GPa)	2.8	ASTM D695
Heat deflection temperature (°C)	53.0	ASTM D648

Historically, one of the earliest methods for determining T_g was by noting the heat deflection temperature of a cast epoxy bar. The data shown in Table 1 were for the tests under 23 °C and the corresponding specimens were cured for 7 days under room conditions. Validation of mechanical properties shown in Table 1 has been carried out. Our measured tensile strength of the epoxy was 13.2 MPa and the corresponding Young's Modulus was 2.8 GPa under the same cure and testing conditions as shown in Table 1. In this paper, the tensile strength and the Young's modulus of this epoxy under different conditions were characterized using Type I dumbbell shaped samples in accordance to ASTM D638. The shape of specimen is shown in Fig. 3.

3.2. Moisture conditioning and temperature levels

All specimens, including both concrete and epoxy, were cured for 28 days at ambient temperature before moisture conditioning. After curing, all specimens were dried in an oven at 50 °C for 3 days in order to minimize the amount of free water inside the concrete specimen. At this stage, the initial mechanical properties of the specimens were measured. The curing process of both concrete and epoxy adopted in this study fulfills the guidelines provided by the existing standards and manufacturer. The specimens were then continuously moisture-conditioned in a temperature controlled water bath. We considered six durations of moisture-conditioning: 0 (dry), 2, 4, 6, 8 and 10 weeks; and two water bath temperatures: 23 °C and 50 °C. The high temperature conditioning represents a realistic upper bound of service temperature that could be reached in the soffit of reinforced concrete beam (Mays and Hutchinson, 1992). For each condition (moisture duration and water bath temperature), three identical samples were prepared and tested experimentally. The high temperature (50 °C) wet conditioning was conducted in a water bath using a Q-Fog CCT 1100 environmental chamber while room temperature (23 °C) wet conditioning was conducted in a water bath in the laboratory with temperature controls.

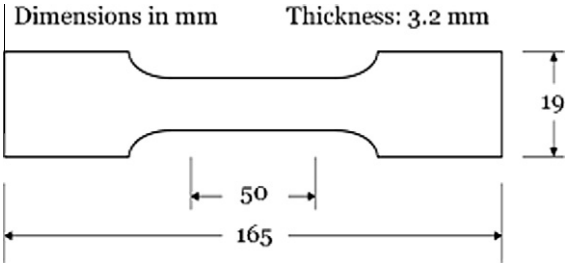

Fig. 3. ASTM D638 Type I dumbbell shaped epoxy tensile specimen.

3.3. Experimental procedure

Compressive tests of concrete were performed on a 60-kip Baldwin machine. Axial strains of the compressive cylinders were measured by means of a pair of clip-on extensometers mounted on opposite sides of the curved surface. The compressive tests were displacement controlled in accordance to ASTM C39.

Mode I fracture tests were performed on an Instron universal test machine Model 1331. The tests were displacement controlled with a rate of 0.1 mm/min (Bazant and Prat, 1988). Fig. 1 shows the schematic diagram of the three-point bending fracture tests for the characterization of the mode I stress intensity factor.

The mode II fracture tests of concrete using the double-edge notched specimens were carried out in the open-loop hydraulic 200-kip Baldwin machine. Fig. 2 shows the schematic testing arrangement. Steel plates with smooth surfaces were placed under and on top of one half of the specimens. The entire arrangement including steel plates and specimen was positioned carefully between the loading platens of the testing machine in order to avoid any possible eccentricity. The load was applied with a constant cross-head displacement rate of 0.3 mm/min (Xu et al., 1995; Reinhardt et al., 1997). Applicability of this specimen geometry and loading arrangement (see Fig. 2) has been shown to generate a shear fracture and to determine the mode II fracture toughness of concrete (Xu et al., 1995; Reinhardt et al., 1997).

Tensile strength and Young's modulus of epoxy were characterized using Type I dumbbell shaped samples (see Fig. 3) with an Instron universal test machine Model 1331 mounted with a 50 kN load cell and a pair of self-tightening grips. Crosshead speed was set at 1 mm/min. A clip-on Instron extensometer with 50 mm gauge length was used to measure the strain within the specimen.

3.4. Calculation of K_I and K_{II} of concrete

The mode I stress intensity factor, K_I, can be obtained from the stress analysis of cracks (Tada et al., 1985) as:

$$K_I = \sigma\sqrt{\pi a}F(a/b), \tag{1}$$

where $\sigma = 6M/b^2$ (stress per unit thickness) in which M is the applied moment, a and b are the crack length and the height of specimen respectively as shown in Fig. 1, and $F(a/b)$ is a configuration correction factor which depends on the ratio a/b (Tada et al., 1985).

The mode II stress intensity factor, K_{II}, derived based on the specimen shown in Fig. 2 can be expressed as (Xu et al., 1995):

$$K_{II} = \frac{\sigma}{4}\sqrt{w}. \tag{2}$$

A uniform compressive stress σ is applied on one half of the specimen with length w.

4. Concrete/epoxy interface

To quantify the interface fracture properties, sandwiched specimens composed of an epoxy layer embedded in a concrete block were used. There are several types of sandwiched specimens which have been used by various researchers, such as, the sandwiched beam specimen for mode I and mixed mode loading tests and the sandwiched Brazilian disk specimen for mixed mode and shear loading tests (Lee and Buyukozturk, 1992, 1995; Trende and Buyukozturk, 1998). For this research, sandwiched beam specimens were chosen to be used in the experiments due to their applicability in studying both the mode I and mixed mode fracture. The analysis of the sandwiched specimens is briefly given as follows.

In the characterization of a bi-material system, the Dundurs parameters α and β, the oscillation index ε, and the shift angle in a sandwiched specimen ω for the bi-material combinations are used (Dundurs, 1969). These parameters are non-dimensional quantities which are the combinations of the elastic moduli of the two materials. In general, α is close to one while β is close to zero in the case of a concrete/epoxy bi-material system.

We consider the four-point bending specimen with a sandwiched epoxy layer shown in Fig. 4. Proper techniques are required to sandwich an epoxy layer between two concrete blocks and create a perfect pre-crack at the interface. The apparent stress intensity factor K_I can be obtained by Tada et al. (1985)

$$K_I = f_1\sigma_r\sqrt{\pi a}, \tag{3}$$

where $\sigma_r = 6M/bd^2$ in which M is the applied moment, a is the crack length, b is the width and d is the height of the specimen. Here, f_1 is a correction factor for four-point pure bending which can be expressed in terms of the relative crack length (a/d):

$$f_1 = 1.122 - 1.4\left(\frac{a}{d}\right) + 7.33\left(\frac{a}{d}\right)^2 - 13.08\left(\frac{a}{d}\right)^3 + 14.0\left(\frac{a}{d}\right)^4. \tag{4}$$

With the assumption that $\beta = 0$, the complex form of the interface stress intensity factors (Suo and Hutchinson, 1989) can be simplified to obtain:

$$K_1 = \sqrt{1-\alpha}(f_1\sigma_r\cos\omega)\sqrt{\pi a} \quad \text{and}$$
$$K_2 = \sqrt{1-\alpha}(f_1\sigma_r\sin\omega)\sqrt{\pi a}. \tag{5}$$

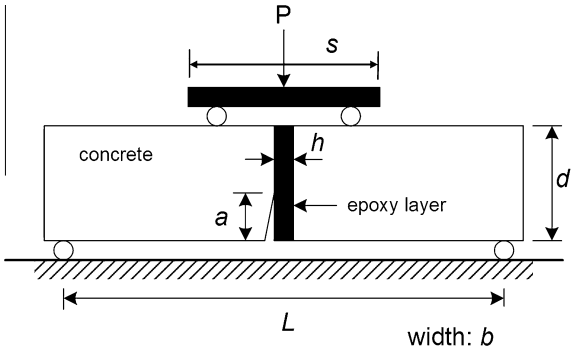

Fig. 4. Sandwiched four-point bending specimen.

The corresponding mode I fracture energy release rate can be calculated as

$$G = \frac{K_I^2}{\bar{E}_1} = \frac{f_1^2 \sigma_r^2 \pi a}{\bar{E}_1}, \tag{6}$$

where $\bar{E}_1$ is the Young's modulus of the concrete substrate under plain strain condition.

Since the specimen is under pure bending condition, the phase angle (Ψ) can be calculated using the following equation (Suo and Hutchinson, 1989; Lee and Buyukozturk, 1992, 1995; Trende and Buyukozturk, 1998):

$$\psi = \omega + \varepsilon \ln\left(\frac{L}{h}\right). \tag{7}$$

The calculated Ψ is in the range of 0–15° which is small, and thus, the specimen can be considered to be essentially in mode I.

Next, the four-point shear specimen shown in Fig. 5 is considered. This specimen has been rigorously analyzed for mixed mode fracture testing (Suo and Hutchinson, 1989). For the four-point shear specimen, the apparent stress intensity factors related to the loads and specimen geometry are given by

$$K_{\mathrm{I}} = \frac{M}{bd^{3/2}} f_b\left(\frac{a}{d}\right), \tag{8}$$

$$K_{\mathrm{II}} = \frac{Q}{bd^{1/2}} f_s\left(\frac{a}{d}\right), \tag{9}$$

where f_b and f_s are correction factors depending on the ratio a/d (He et al., 1990). M and Q and the applied moment and shear force at the crack location respectively, and b_1, b_2 and d are geometric quantities defined in Fig. 5.

Again, with the assumption that $\beta = 0$, the complex form of the interface stress intensity factors (Suo and Hutchinson, 1989) can be simplified to obtain:

$$K_1 = \sqrt{1-\alpha}(K_{\mathrm{I}} \cos\omega - K_{\mathrm{II}} \sin\omega) \quad \text{and}$$
$$K_2 = \sqrt{1-\alpha}(K_{II} \cos\omega + K_I \sin\omega). \tag{10}$$

The corresponding energy release rate can be calculated as

$$G = \frac{K_I^2 + K_{II}^2}{\bar{E}_1}. \tag{11}$$

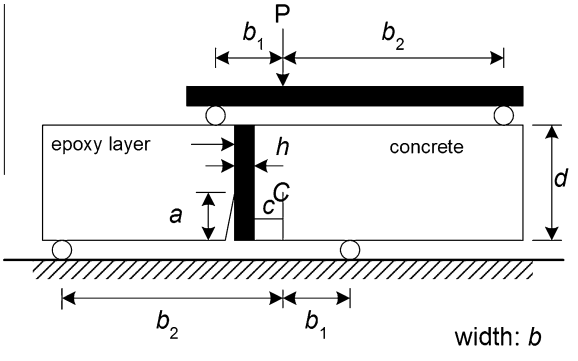

Fig. 5. Sandwiched four-point shear specimen.

To determine the loading angle (ϕ) for the four-point shear test, the following equation can be used: $\phi = \tan^{-1}(f_s d/f_b c)$. However, the phase angle (Ψ) also depends on the material combinations. In this study, the value of α is not constant because it depends on the Young's modulus of the constituent materials which changes with the moisture content. As a result, ω also changes with the moisture content. By considering all cases with different duration of moisture conditioning, it is noticed that the value of α and ω did not vary significantly and the mean shift of 11° was taken into account.

In order to calculate the interface fracture toughness, the material properties of individual materials need to be known. These are the Young's modulus of concrete and epoxy, and their Poisson's ratio (ν), which are used in the calculation of the Dundurs parameters α and β, the oscillation index ε, and the shift angle in a sandwiched specimen ω. The Poisson's ratio was assumed to be 0.2 for concrete (Oluokun et al., 1988) and 0.35 for epoxy (Tschoegl et al., 2002), while the Young's modulus of constituent materials was measured experimentally as related to various moisture and temperature values. It should be noted that α and β are not constants because Young's modulus of both concrete and epoxy decreases with increasing moisture content. It is worth to mention that the value of β was still about 0.1 (close to zero) throughout the concerned moisture duration. This implies that the assumption which considers $\beta = 0$ is reasonable. After calculating the value of α and β, the procedure shown above can be used for evaluating the fracture toughness at the concrete/epoxy interface under mode I and mixed mode loading conditions.

4.1. Specimens

To generate the fracture toughness for both mode I and mixed mode conditions, the two types of sandwiched beam specimens presented above were tested. Each sandwiched beam specimen was manufactured by casting and joining two concrete blocks. These blocks had the same cross sectional dimension with 76.2 mm (height) × 38.1 mm (thickness), but their lengths were different. One was 152.4 mm long; while the other was 228.6 mm long. These concrete blocks were all properly cured and then dried in order to ensure the concrete faces, onto which epoxy would be applied, was dry when they were bonded.

The thickness of the epoxy layer, h, was 2.54 mm for both specimens. The thickness of this layer is chosen at least one order of magnitude smaller than the dimension of the specimen such that linear elastic fracture mechanics is applicable, and the energy release rate of the specimen can be evaluated based on the Young's modulus of concrete only. The relative crack size (a/d) was 0.5 for all the specimens. In this study, L = 228.6 mm and s = 114.3 mm (see Fig. 4); while b_1 = 139.7 mm in, b_2 = 88.9 mm, c = 5 mm (see Fig. 5). Grade 40 normal strength concrete with an average 28-day compressive strength of 38 MPa and the epoxy which was characterized in the previous section were used. To ensure that there was a sharp precrack at the interface, a notch plate made of thin plastic with the thickness of 0.1 mm was attached to one side of the epoxy layer.

4.2. Moisture conditioning and temperature levels

The moisture conditioning of sandwiched beam specimens was similar to that described in the previous section. It should be noted that the Dundurs parameters α and β, the oscillation index ε, and the shift angle in a sandwiched specimen ω for the bi-material combination were computed based on the material property characterization of constituent materials corresponding to certain moisture and temperature levels.

4.3. Experimental procedure

Four-point bending and shear tests were performed on the sandwiched beam specimens using an Instron Model 1331 machine with a 50 kN load cell. The point load deflection was measured by an extensometer which was mounted on a reference frame. All tests were carried out under displacement control with a rate of 0.00167 mm/min (He et al., 1990). The phase angle (Ψ) of the bending specimen was assumed to be 0°, while the phase angle (Ψ) of the shear specimen was adjusted to be 60° in order to achieve the desired mixed-mode loading condition.

The tests were stopped when the load dropped below 50% of the peak load. Using the loading procedure outlined above, the peak load was reached within 10 min after the start of the test. During the tests, load and point load deflection were both continuously recorded.

5. Results

Experimental results are presented in a manner that each data point refers to one particular moisture duration as mentioned in Sections 3.2 and 4.2. The mean value of the mechanical property and the mean moisture content were calculated based on three samples under the same moisture and temperature conditioning and were presented as a point in the following plots. The error bars in the plots refer to one standard deviation of the concerned coordinates.

5.1. Constituent materials: concrete and epoxy

The measured compressive strength (f_c') and Young's modulus (E_c) of concrete were 40.9 MPa and 35.5 GPa, respectively before moisture conditioning. Figs. 6 and 7 show, respectively, the variations of compressive strength and Young's modulus with increasing moisture content. Moisture content was measured as a weight difference, $(W_{final} - W_{initial})/W_{initial}$. It should be noted that zero moisture content shown in the figures (dry condition) refers to the stage at which the specimen had been kept in oven at 50 °C for 3 days. Trend lines are given as a result of regression analysis. In general, it is observed that moisture degradation took place in both constituent materials. The degradation of mechanical properties in concrete under moisture can be approached from a viewpoint of volumetric change of the hardened cement pastes. Increase in the volume of hardened cement pastes under moisture and the resulting decrease in the average distance between the surfaces of the hardened cement gel may lead to a decrease in secondary bonds between the surfaces. As a result, the strength for wet specimens may decrease. Strength reduction can be up to 40% as demonstrated from the regression line in Fig. 6. The Young's modulus of concrete, on the other hand, was not affected by much even after 10 weeks of moisture conditioning in a water bath. The results also show that the effect of different conditioning temperatures on the mechanical properties of concrete was not significant. There was less data scattering in Young's modulus when compared with the case of compressive strength. The more scattering of the data found in compressive strength can be attributed to the redundant crack paths that may be available when concrete is subjected to compression, while the Young's modulus was measured at an infant stage prior to significant crack formation.

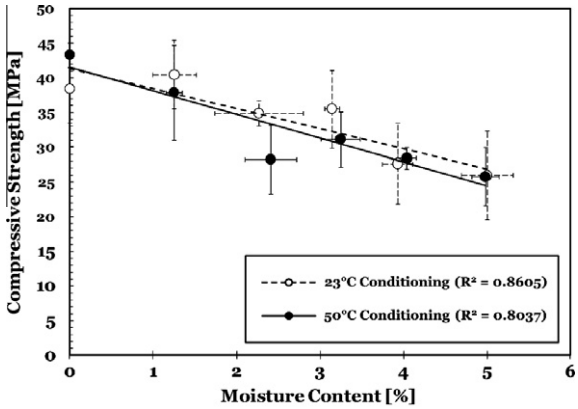

Fig. 6. Concrete compressive strength vs. moisture uptake.

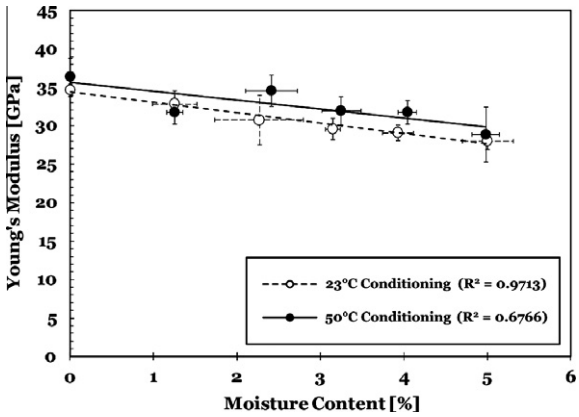

Fig. 7. Young's modulus vs. moisture uptake.

Fig. 8 shows the variation of mode I fracture toughness with increasing moisture uptake. It is observed that fracture toughness reduction ranged from 12% to 15%. Again, the mode I fracture toughness of concrete was not significantly affected by increased temperatures. The scattering of data found in mode I fracture test is less when compared to that in compressive test. This can be explained by the fact that the crack propagation locus under mode I fracture

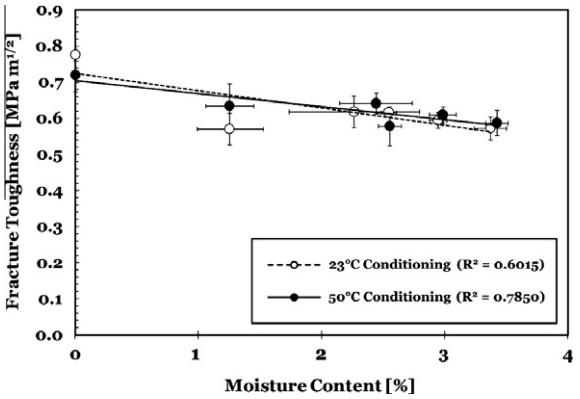

Fig. 8. Concrete mode I fracture toughness vs. moisture uptake.

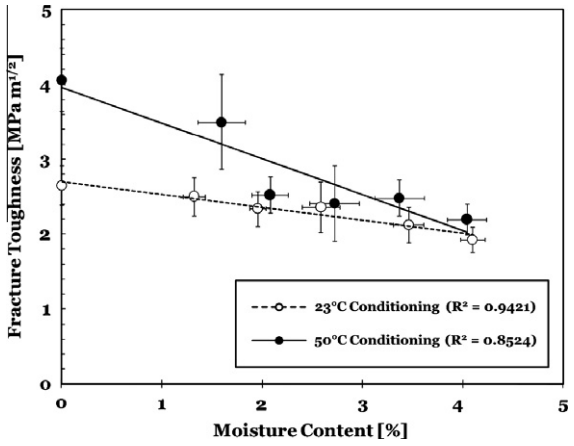

Fig. 10. Concrete mode II fracture toughness vs. moisture uptake.

is relatively clear while redundant crack paths are available in concrete when subjected to compression.

The mode II double-edged notch specimens were carefully examined, especially near the notch. Under the loading condition as shown in Fig. 2, an inclined crack was initiated at the tip of the notch. Fig. 9 shows an example in which crack started at the notch tip and merged in the unloaded part. The critical stress corresponding to the shear crack initiation was used for the computation of mode II fracture toughness of concrete K_{IIc}. The mode II fracture toughness of concrete was plotted against the moisture content in Fig. 10. The decrease in mode II fracture toughness was approximately 27% and 48% for 23 °C and 50 °C temperature groups, respectively, after 8 weeks of moisture conditioning. It was observed that the reduction of mode II fracture toughness of concrete is more than that of mode I, especially at higher temperature.

The explanation of the reduction in fracture toughness can be made from a viewpoint of internal pore water pressure (Bazant and Thonguthai, 1978). It is believed that the internal pore water pressure is developed in wet concrete under external loading due to the limited pore space. Migration of water in a pore is not allowed when adjacent pores are also filled with water. Due to the capillary actions, the hindered adsorbed water produces a very high disjoining pressure between the contacting cement pastes. This pressure is expected to be responsible for intensifying the stress intensities at the micro-crack tips leading to earlier crack propagation under external loading. As a result, the fracture resistance of wet concrete becomes lower, as compared to that of dry concrete.

Figs. 11 and 12 show the variations of tensile strength and Young's modulus of epoxy with increasing moisture content, respectively. It is observed that both tensile strength and Young's modulus decreased with moisture content. This result is consistent with our understanding of polymer behavior and is in line with the current literature. The decrease in these mechanical properties upon immersion is due to plasticization (Moy and Karasz, 1980) and, possibly, to hydrolysis processes (May, 1988; Fromonteil et al., 2000). It is noted that both the tensile strength and the stiffness decreased drastically under 50 °C when compared to the mechanical properties under 23 °C; the Young's modulus measured at 50 °C did not appear sensitive to the duration of moisture conditioning. It is suggested that a moderate immersion temperature (50 °C) is able to enhance the plasticization effect brought

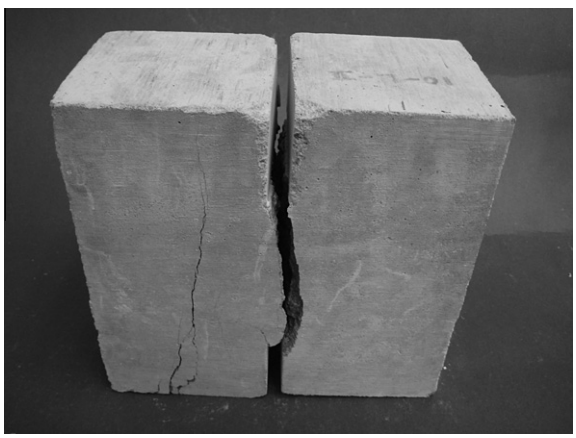

Fig. 9. Crack pattern of double-edged notch specimen.

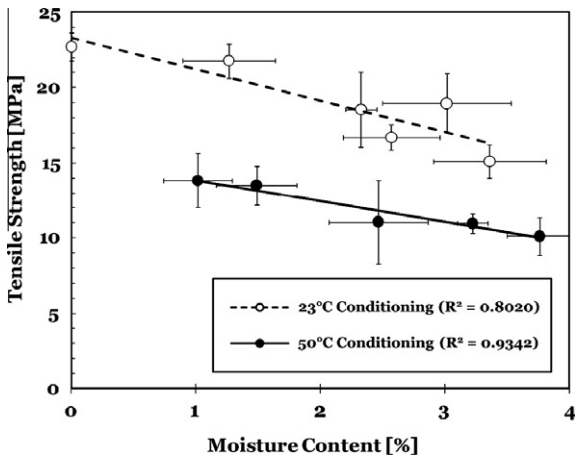

Fig. 11. Epoxy tensile strength vs. moisture uptake.

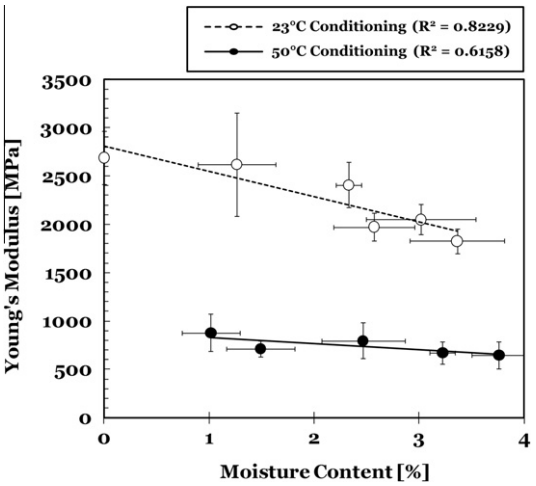

Fig. 12. Epoxy Young's modulus vs. moisture uptake.

about by the water penetrating epoxy (Browning, 1978; May, 1988). It should be mentioned that the initial tensile strength of epoxy after the thermal treatment at 50 °C for 3 days was higher than that measured after the cure performed at room temperature (23 °C) for 7 days while the Young's modulus of epoxy measured after these two different treatments did not show any significant changes. Thus, the Young's modulus of the studied epoxy did not appear sensitive to the rise in temperature when temperature in that range is the only varying parameter.

It is found that compressive strength, stiffness, mode I and mode II fracture toughnesses of concrete decrease at a similar rate under moisture conditioning. The results found in the mechanical property characterization of concrete agreed with the previously reported work, mostly available for compression and mode I fracture properties (Bazant and Thonguthai, 1978; Bazant and Prat, 1988; Ross et al., 1996; Konvalinka, 2002). Thus, the experimental results validated the degradation of mechanical properties in concrete when subjected to moisture ingress.

5.2. Concrete/epoxy interface

Equipped with the quantitative mechanical property characterization of concrete and epoxy, the interface fracture toughness can now be quantified based on the methodology described previously.

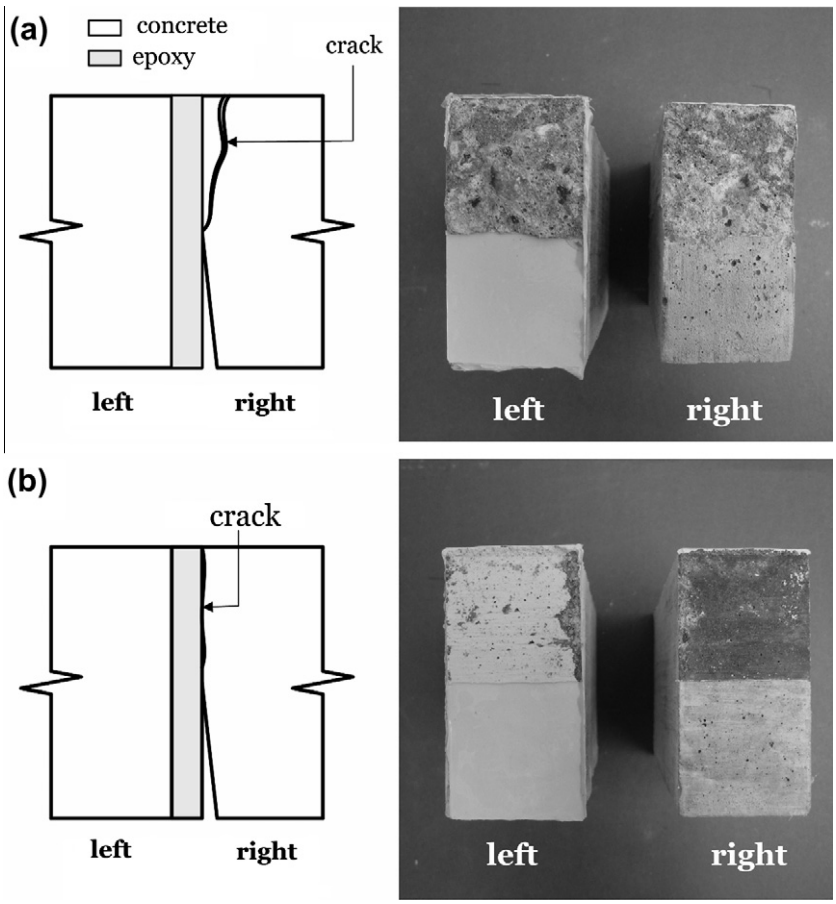

Fig. 13. (a) Concrete delamination of bending beam specimen under dry condition and (b) interface separation of bending beam specimen after 4-week moisture conditioning.

Typical failure modes of the sandwiched bending beam specimens with and without moisture conditioning are shown in Fig. 13. Fig. 13(a) shows the failure mode of the dry sandwiched bending specimen at 23 °C. Fig. 13(b) shows the failure mode of the wet sandwiched bending specimen with 4-week moisture duration at 50 °C.

Dry bending beam specimens exhibited failure in concrete itself, rendering a cohesive type of failure. The precrack, which was placed at the concrete/epoxy interface, kinked into the concrete upon reaching the peak load. The specimen failed by concrete delamination. This phenomenon was observed for both temperature groups. Failure surface was felt powdery to the touch and small grains of sand were clearly seen at the failure surface.

Wet sandwiched bending beam specimens, on the other hand, exhibited a distinctive concrete/epoxy interface separation. For the specimens under moisture conditioning of 2 weeks and 4 weeks, a relatively small amount of loose concrete particles adhered to the epoxy layer. However, for the specimen under moisture conditioning over 4 weeks, a clear separation between concrete and epoxy was observed. It was noted that the crack did not kink into concrete substrate at all during the entire testing process, but remained propagating along the moist concrete/epoxy interface. It is observed that the shift of fracture failure mode from concrete delamination to interface separation is accompanied by the substantial decrease of the mode I interface fracture toughness.

The variations of mode I fracture toughness (phase angle is close to 0°) under different moisture durations are shown in Figs. 14(a) and (c). For each moisture and temperature condition, the corresponding fracture toughness was the average among three tested specimens. It is observed that there was a decrease in the interface fracture toughness and an asymptotic behavior can be achieved with increasing moisture ingress. In particular, there was a substantial decrease in fracture energy release rate with a complex phenomenon which involves a distinctive dry-to-wet debonding mode shift from material decohesion (concrete delamination) to interface separation. This level of deterioration occurred after 4 weeks of moisture conditioning at 23 °C while after 2 weeks of moisture conditioning at 50 °C. This reveals that the combined effect of moisture and high temperature may produce a more severe deterioration.

Upon closer examination of the tested specimens failing by interface separation, it was observed that there was a dark color at the crack face of the concrete block (Fig. 13) showing that moisture penetrated into the interface leading to a significant change in failure mechanism. Also, when compared to the deterioration of constituent materials under moisture and temperature effects, the deterioration of the concrete/epoxy interface is seen to be more severe. This implies that the durability of the individual constituent material cannot be solely used to extrapolate to the durability of a bi-material bonded system.

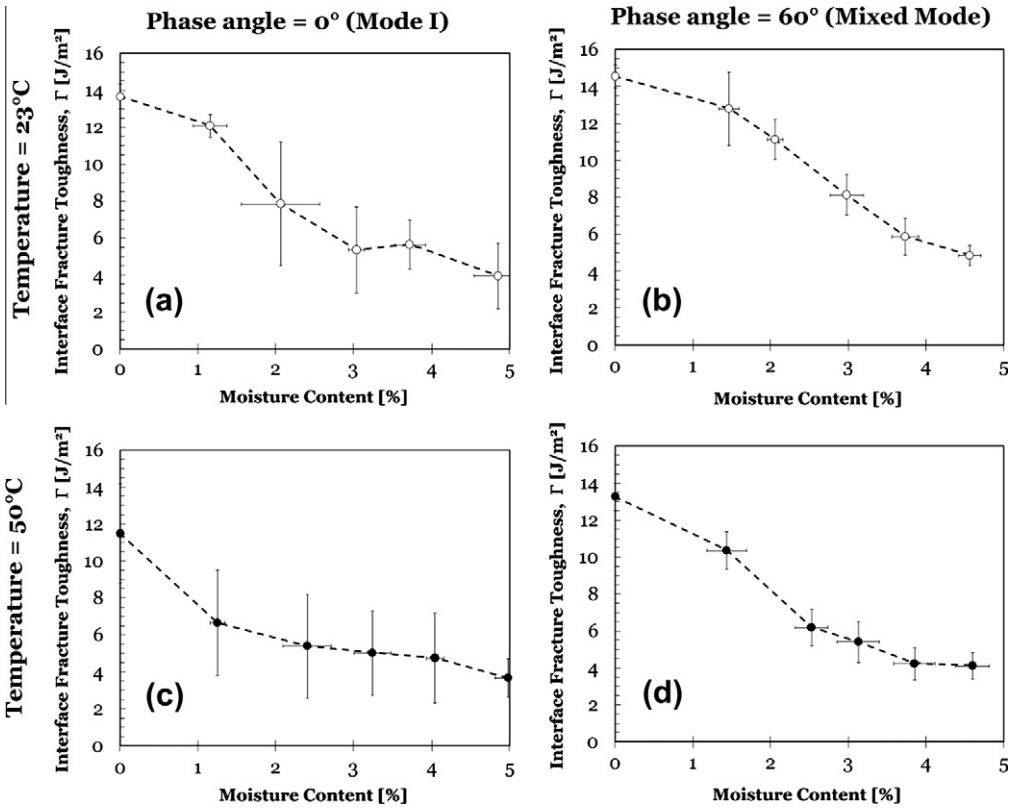

Fig. 14. Mode I and mixed mode interface fracture toughness variation under two different temperatures.

Unlike the pure bending specimen, the failure mechanism in the mixed mode case did not change from dry to wet condition. The variation of the mixed mode fracture toughness when subjected to different moisture durations and temperatures are shown in Figs. 14(b) and (d). The fracture toughness at each condition is the average among the three tested specimens. It is observed that there is a decreasing trend for both temperature groups in the mixed mode fracture toughness with increasing moisture duration, however, with a slower rate when compared with the variation of mode I interface fracture toughness.

The mixed mode fracture toughness of all wet specimens showed some degradation over time between the 2-week and 10-week test periods. In particular, high temperature conditioning group started to degrade severely after 4 weeks. Fracture toughness degraded by approximately 50% after 8 weeks under 23 °C. In the mixed mode fracture case, the duration for the asymptotic behavior was much longer because the entire bond contributed to the debonding resistance, as opposed to the length of few centimeters near the crack tip in mode I fracture.

6. Crack kinking behavior

Recent research works using MDCB experiment have been carried out for quantifying the interface fracture toughness (Ouyang and Wan, 2008, 2009). Although the tests captured the variation of the interface fracture toughness and the shift of failure mode, they resulted in a very large magnitude of the interface fracture toughness leading to a failure in explaining the shift in failure mode by kink criterion. We believe that the present work provides a robust experimental method in quantifying the interface fracture toughness and the results show that the kink criterion can be used to explain the shift of failure mode in a quantitative way, rather than explaining the phenomenon qualitatively.

Under mode I fracture loading condition, the locus of fracture for all dry cases stayed within the concrete substrate. The parent pre-crack at the concrete/epoxy interface that was generated by a thin Teflon film kinked into the concrete substrate and subsequent crack propagation stayed close and parallel to that interface. This led to a thin layer of concrete adhered to the debonded strip. The locus of fracture for all wet cases, on the other hand, occurred at the concrete/epoxy interface, staying along the same path as that of the pre-crack. In other words, no kinking was observed.

To study the shift in crack kinking behavior, the kink criterion (He and Hutchinson, 1989) is employed. The kink criterion states that when

$$\frac{\Gamma_i}{\Gamma_s} > \frac{G_i}{G^t_{\max}} \tag{12}$$

is satisfied, the parent crack that lies at the interface of the two adjoining materials will tend to kink into the substrate in consideration. Here, Γ_i, is the interface fracture toughness, Γ_s, the substrate fracture toughness in mode I, G_i the interface fracture energy release rate (of the parent crack), and $G^t_{\max}$ the maximum fracture energy release rate for the kink crack at any putative kink angle. It should be mentioned that Γ_s is defined as K^2_{IC}/E where K_{IC} is the critical stress intensity factor and E is the Young's modulus so that the unit of Γ_s is the same as that of Γ_i as defined in this paper. One should note that the ratio is less than unity because G_i is always less than $G^t_{\max}$, due to the definition of G_i.

When dry, the epoxy exhibited a concrete delamination mode of debonding and the corresponding mode I interface fracture toughness was roughly 14 J/m^2. Since debonding did not occur at the interface, the actual toughness values of the concrete/epoxy interface were higher than those values. Considering the mode I fracture toughness values of concrete (oven-dried) as presented before, Γ_s is about 13 J/m^2 and thus Γ_i/Γ_s is greater than 1. Recalling that $G_i/G^t_{\max}$, has a value of less than unity, it is noted that the expression (12) was satisfied. The kink criterion thus predicts that the parent pre-crack would kink into the concrete substrate. This prediction is inline with the observed failure mode where concrete delamination took place in both loading configurations.

Although the kink criterion is capable in predicting the initial crack propagation tendency, it fails to provide further insight regarding the subsequent crack front behavior. In other words, the kink criterion explains why the pre-crack kinked into the concrete substrate, but it does not indicate why the crack continued to propagate close and parallel to the concrete/epoxy interface, rather than penetrating deeper into the supposedly brittle concrete block.

When wet, all mode I fracture specimens exhibited a consistent interface separation mode at the concrete/epoxy interface when the moisture duration was equal to or longer than 4 weeks. The corresponding mode I interface fracture toughness was roughly 4 J/m^2. Since debonding occurred at the interface, the measured values were the actual toughness values of the concrete/epoxy interface. Again, considering the mode I fracture toughness values of concrete (oven-dried) as presented above, it is found that Γ_s is about 10 J/m^2 and thus Γ_i/Γ_s is smaller than 1 which implies the expression (12) may not be satisfied. The kink criterion thus predicts that the parent pre-crack would not kink into the concrete substrate. Since the epoxy materials had a mode I fracture toughness with variation in a high range, based on the existing lab data, crack kinking into the epoxy layer was unlikely to occur. As a result, the crack should propagate along the interface as it could not kink into either material. This prediction is inline with the observed failure mode where a clear interface separation took place.

In all mixed mode fracture specimens, the standard criterion for crack kinking out of an interface cannot be used to predict the kinking angle. No matter how the interface fracture toughness reduced in the concrete/epoxy bi-material, the kinking direction was always to be approximately perpendicular to the direction of maximum tensile stress in the sandwiched beam specimens. It is observed that kinking always ended at the bearing of the main load, and hence the kinking angle is determined by the loading geometry. Further studies on kink criterion under mixed mode condition should be carried out. The mixed mode loading geometry is a possible parameter influencing the direction of the crack propagation.

7. Discussion

With the interface fracture properties quantified as reported in this paper, computational modeling of a structure involving FRP-bonded concrete systems may become feasible. In such a fracture-based modeling, cohesive elements can be used with interface fracture properties as affected by different levels of moisture. Also, the mechanical properties for the constituent materials characterized in this study can be adopted in such an analysis. Thus, through the simulation of large-scale FRP-bonded concrete systems, such as a composite beam, one can demonstrate how the local deterioration at the interface may affect the structural integrity of the system.

The moisture effect on concrete and epoxy may result in the degradation of mechanical properties, such as tensile and compressive strength, and fracture toughness, with a reduction amounting up to approximately 40%. However, the moisture effect on the interface properties may be much more severe. In this case, there may be a shifting in debonding mode from material decohesion to interface separation under prolonged moisture conditioning. This mechanism is complicated. Two explanations of the shift in debonding mode can be given. One may be the plasticization, that is the formation of a layer of epoxy-penetrated concrete; and the other may be the weakening of the adhesive force between concrete and epoxy due to their physical and chemical interactions in the presence of water molecules. A better understanding can be developed through a more fundamental study at the atomistic level using a molecular dynamics approach.

8. Conclusion

A fundamental study on the interface fracture of concrete/epoxy systems under the effect of moisture was performed. Mechanical properties of constituent materials, both concrete and epoxy, were measured under the influence of accelerated moisture ingress. Interfacial property was quantified using the concept of interface fracture toughness. Moisture acceleration is facilitated through continuous conditioning under water bath at elevated temperature. Test results reveal that moisture is generally detrimental to the strength, the stiffness and the fracture toughness of the constituent materials. However, the moisture effect on the deterioration of the interface fracture toughness is more severe. Such deterioration is accompanied by a shifting in failure mode from concrete delamination to interface separation under mode I loading condition.

The detrimental effect of moisture on the interface of the bonded system found in this study was inline with other limited numbers of independent studies conducted on FRP retrofitted concrete beams. The quantitative knowledge and data provided through this work on fracture properties of concrete/epoxy interface will allow the establishment of the relationship between local interface deterioration and global behavior of FRP-bonded structures as a basis for life-cycle prediction. For this purpose, it is recommended that parametric studies on FRP-bonded concrete beams should be made through appropriate finite element models incorporating cohesive interface elements. Furthermore, there is a need to conduct a more fundamental study of the observed shift in debonding mode from the concrete delamination to the interface separation through understanding of the physical and chemical interactions among the constituent materials in the presence of water molecules. Hence, a numerical simulation using the concept of molecular dynamics is recommended.

References

Au, C., Büyüköztürk, O., 2006a. Peel and shear fracture characterization of debonding in FRP plated concrete affected by moisture. Journal of Composites for Construction ASCE 10 (1), 35–47.

Au, C., Büyüköztürk, O., 2006b. Debonding of FRP plated concrete: a tri-layer fracture treatment. International Journal of Engineering Fracture Mechanics 73, 348–365.

Bazant, Z.P., Thonguthai, W., 1978. Pore pressure and drying of concrete at high temperature. Proceedings ASCE 104 (EM5), 1059–1079.

Bazant, Z.P., Prat, P.C., 1988. Effect of temperature and humidity on fracture energy of concrete. ACI Materials Journal 85 (4), 262–271.

Browning, C.E., 1978. The mechanisms of elevated temperature property losses in high performance structural epoxy resin matrix materials after exposures to high humidity environments. Polymer Engineering & Science 18, 16–24.

Buyukozturk, O., Hearing, B., 1998a. Failure behavior of precracked concrete beams retrofitted with FRP. Journal of Composites for Construction ASCE 2 (3), 138–144.

Buyukozturk, O., Hearing, B., 1998b. Crack propagation in concrete composites influenced by interface fracture parameters. International Journal of Solids and Structures 35 (31–32), 4055–4066.

Buyukozturk, O., Gunes, O., Karaca, E., 2004. Progress on understanding debonding problems in reinforced concrete and steel members strengthened using FRP composites. Construction and Building Materials 18 (1), 9–19.

Coronado, C.A., Lopez, M.M., 2008. Experimental characterization of concrete–epoxy interfaces. Journal of Materials in Civil Engineering ASCE 20 (4), 303–312.

Dundurs, J., 1969. Edge-bonded dissimilar orthogonal elastic wedges. Journal of Applied Mechanics 36, 650–652.

Fromonteil, C., Bardelle, Ph., Cansell, F., 2000. Hydrolysis and oxidation of an epoxy resin in sub- and supercritical water. Industrial & Engineering Chemistry Research 39 (4), 922–925.

Frigione, M., Aiello, M.A., Naddeo, C., 2006. Water effects on the bond strength of concrete/concrete adhesive joints. Construction and Building Materials 20, 957–970.

Giurgiutiu, V., Lyons, J., Petrou, M., Laub, D., Whitley, S., 2001. Fracture mechanics testing of the bond between composite overlays and a concrete substrate. Journal of Adhesion Science and Technology 15 (11), 1351–1371.

Gunes, O., Buyukozturk, O., Karaca, E., 2009. A fracture-based model for FRP debonding in strengthened beams. Engineering Fracture Mechanics 76 (12), 1897–1909.

He, M.Y., Hutchinson, J.W., 1989. Kinking of a crack out of an interface. Journal of Applied Mechanics 56, 270–278.

He, M.Y., Cao, H.C., Evans, A.G., 1990. Mixed-mode fracture: the four-point shear specimen. Acta Metallurgica Materialia 38 (5), 839–846.

Karbhari, V.M., Engineer, M., 1996. Investigation of bond between concrete and composites: use of a peel test. Journal of Reinforced Plastics and Composites 15 (2), 208–227.

Karbhari, V.M., Engineer, M., Eckel II, D.A., 1997. On the durability of composite rehabilitation schemes for concrete: use of a peel test. Journal of Material Science 32 (1), 147–156.

Konvalinka, P., 2002. Effect of Moisture Content of Concrete Specimen on its Stress–Strain Diagram in Compression. CTU Reports, vol. 6, No. 2, Czech Technical University in Prague, pp. 59–66.

Lau, D., Buyukozturk, O., 2009. Moisture degradation in concrete/epoxy systems. In: Proceedings of FRPRCS-9, Sydney, Australia, 2009.

Lee, K.M., Buyukozturk, O., 1992. Fracture analysis of mortar-aggregate interfaces in concrete. Journal of Engineering Mechanics ASCE 118 (10), 2031–2047.

Lee, K.M., Buyukozturk, O., 1995. Fracture toughness of mortar-aggregate interface in high-strength concrete. ACI Material Journal 92 (6), 634–642.

May, C.A., 1988. Epoxy Resin: Chemistry and Technology, second ed. Marcel Dekker Ltd., New York, NY.
Mays, G.C., Hutchinson, A.R., 1992. Adhesives in Civil Engineering. Cambridge University Press, UK.
Moy, P., Karasz, F.E., 1980. Epoxy–water interactions. Polymer Engineering & Science 20, 315–319.
Oluokun, F.A., Burdette, E.G., Deatherage, J.H., 1988. Elastic modulus, Poisson's ratio, and compressive strength relationships at early ages. ACI Materials Journal 88 (1), 3–10.
Ouyang, Z., Wan, B., 2008. Experimental and numerical study of moisture effects on the bond fracture energy of FRP/concrete joints. Journal of Reinforced Plastics and Composites 27 (2), 205–223.
Ouyang, Z., Wan, B., 2009. Nonlinear deterioration model for bond interfacial fracture energy of FRP-concrete joints in moist environments. Journal of Composites for Construction ASCE 13 (1), 53–63.
Qiao, P., Xu, Y., 2004. Evaluation of fracture energy of composite–concrete bonded interfaces using three-point bend tests. Journal of Composites for Construction ASCE 8 (4), 352–359.
Reinhardt, H.W., Ozbolt, J., Xu, S., Dinku, A., 1997. Shear of structural concrete members and pure mode II testing. Advanced Cement Based Materials 5, 75–85.
Reinhardt, H.W., Xu, S., 1998. Experimental determination of K_{IIc} of normal strength concrete. Materials and Structures 31, 296–302.
Ross, C.A., Jerome, D.M., Tedesco, J.W., Hughes, M.L., 1996. Moisture and strain rate effects on concrete strength. ACI Materials Journal 93 (3), 293–300.
Smith, S.T., Teng, J.G., 2001. Interfacial stresses in plated beams. Engineering Structures 23 (7), 857–871.
Suo, Z., Hutchinson, J.W., 1989. Sandwich test specimens for measuring interface crack toughness. Materials Science and Engineering A107, 135–143.
Tada, H., Paris, P.C., Irwin, G.R., 1985. The Stress Analysis of Cracks Handbook, second ed. Paris Productions Incorporated (and Del Research Corporation), St Louis, MO.
Taljsten, B., 1996. Strengthening of concrete prisms using the plate-bonding technique. International Journal of Fracture 82, 253–266.
Teng, J.G., Chen, J.F., Smith, S.T., Lam, L., 2002. FRP-Strengthened RC Structures. Wiley-VCH, John Wiley & Sons, Ltd., Chichester, UK.
Trende, U., Buyukozturk, O., 1998. Size effect and influence of aggregate roughness in interface fracture of concrete composites. ACI Materials Journal 95 (4), 331–338.
Tschoegl, N.W., Knauss, W.G., Emri, I., 2002. Poisson's ratio in linear viscoelasticity – a critical review. Mechanics of Time-Dependent Materials 6 (1), 3–51.
Wan, B., Petrou, M.F., Harries, K.A., 2006. Effect of the presence of water on the durability of bond between CFRP and concrete. Journal of Reinforced Plastics and Composites 25 (8), 875–890.
Xu, S., Reinhardt, H.W., Gappoev, M., 1995. Mode II fracture testing method for highly orthotropic materials like wood. International Journal of Fracture 75 (3), 185–214.
Yuan, H., Teng, J.G., Seracino, R., Wu, Z.S., Yao, J., 2004. Full-range behavior of FRP-to-concrete bonded joints. Engineering Structures 26 (5), 553–565.